

Published in final edited form as:

*J Am Chem Soc.* 2013 June 12; 135(23): 8692–8701. doi:10.1021/ja4029507.

## Insights into the Mechanism of Peptide Cyclodehydrations Achieved Through the Chemoenzymatic Generation of Amide Derivatives

Kyle L. Dunbar<sup>1,2</sup> and Douglas A. Mitchell<sup>1,2,3,\*</sup>

<sup>1</sup>Department of Chemistry, University of Illinois at Urbana Champaign, Urbana, Illinois, USA.

<sup>2</sup>Institute for Genomic Biology, University of Illinois at Urbana Champaign, Urbana, Illinois, USA.

<sup>3</sup>Department of Microbiology, University of Illinois at Urbana-Champaign, Urbana, Illinois, USA.

### Abstract

Current strategies for generating peptides and proteins bearing amide carbonyl derivatives rely on solid-phase peptide synthesis for amide functionalization. Although such strategies have been successfully implemented, technical limitations restrict both the length and sequence of the synthetic fragments. Herein we report the repurposing of a thiazole/oxazole-modified microcin (TOMM) cyclodehydratase to site-specifically install amide backbone labels onto diverse peptide substrates, a method we refer to as azoline-mediated peptide backbone labeling (AMPL). This convenient chemoenzymatic strategy can generate both thioamides and amides with isotopically labeled oxygen atoms. Moreover, we demonstrate the first leader peptide-independent activity of a TOMM synthetase, circumventing the requirement that sequences of interest be fused to a leader peptide for modification. Through bioinformatics-guided site-directed mutagenesis, we also convert a strictly dehydrogenase-dependent TOMM azole synthetase into an azoline synthetase. This vastly expands the spectrum of substrates modifiable by AMPL by allowing any *in vitro* reconstituted TOMM synthetase to be employed. To demonstrate the utility of AMPL for mechanistic enzymology studies, an <sup>18</sup>O-labeled substrate was generated to provide direct evidence that cyclodehydrations in TOMMs occur through the phosphorylation of the carbonyl oxygen preceding the cyclized residue. Furthermore, we demonstrate that AMPL is a useful tool for establishing the location of azolines both on *in vitro* modified peptides and azoline-containing natural products.

### INTRODUCTION

Stable amide labels are gaining prominence in the field of chemical biology as probes that minimally perturb polypeptide/structure and electronics at the site of installation. For example, <sup>17</sup>O- and <sup>18</sup>O- labeled amides are useful probes for the study of polypeptide dynamics by NMR and time-resolved 2D-IR, respectively.<sup>1-7</sup> Thioamides, on the other hand, have garnered significant attention due to their ability to increase the protease stability of peptides, restrict conformational flexibility around the amide bond, photoisomerize from *trans* to *cis* upon excitation with 260 nm light, and act as minimal fluorescence quenchers for protein folding studies.<sup>8-12</sup> While the utility of such labels is continually expanding, the

\*Corresponding Author; (douglasm@illinois.edu), phone: 1-217-333-1345, fax: 1-217-333-0508 .

Supporting Information Additional experimental procedures, supporting figures as mentioned in text. This information is available free of charge via the Internet at <http://pubs.acs.org>.

The authors declare no competing financial interest.

backbone-incorporation techniques for these labels are currently limited to solid-phase peptide synthesis (SPPS).<sup>1-8,10-13</sup>

This process is expensive and time-consuming, as the generation of labeled residues must be done prior to SPPS, and also suffers from all the limitations of SPPS (*e.g.* peptide length and sequence restrictions). An alternative approach that would obviate the requirement for SPPS would be heterologous expression and purification of the desired polypeptide/protein followed by the posttranslational installation of the backbone label. Our previous work in peptide heterocyclization chemistry has suggested a route for installing oxygen isotopes and thioamides into polypeptide/proteins using the azoline heterocycle as an entry point.

Thiazoline and (methyl)oxazoline heterocycles are posttranslationally installed in the thiazole/oxazole-modified microcin (TOMM) class of peptidic natural products. These rings are formed from the cyclization of Cys, Ser and Thr residues onto the preceding amide carbonyl. Although the precise mechanism has yet to be fully elucidated, it is known that a two-protein cyclodehydratase complex (C and D proteins) performs the ATP-dependent cyclization of select residues to afford azoline heterocycles (Figure 1).<sup>14,15</sup> In the majority of TOMM natural products, a flavin mononucleotide (FMN)-dependent dehydrogenase (B protein) catalyzes the two-electron oxidation of the nascent rings to afford the aromatic azoles.<sup>14,16</sup> In cases where oxidation does not occur, the azolines are often either sterically or electronically protected from nucleophiles (*e.g.* thiostrepton, ulithiacyclamide, and plantazolicin; Figure S1).<sup>17-19</sup> As azolines lack the aqueous stability of their aromatic counterparts,<sup>20-22</sup> the dearth of unprotected azoline heterocycles in characterized TOMMs likely represents an evolutionary bias for compounds with increased stability. Even so, azoline-containing TOMM natural products have been reported to undergo partial hydrolysis during purification.<sup>19</sup> Based on the susceptibility of azoline heterocycles towards nucleophilic attack, we hypothesized that azoline heterocycles could be used as moieties for the site-selective modification of peptide backbones.

Recently, we reported on the characterization of a TOMM synthetase from *Bacillus* sp. Al Hakam (Balh), and demonstrated that the Balh cyclodehydratase is catalytically competent in the absence of the associated dehydrogenase.<sup>23,24</sup> This enzyme complex had exceptional *in vitro* activity and a predictable set of rules for the modification of diverse substrates.<sup>23</sup> Coupling the promiscuous, yet highly predictable, nature of heterocyclization by the Balh cyclodehydratase with the lability of azoline heterocycles, we report a convenient and robust chemoenzymatic strategy for the site-selective installation of thioamides and isotopically labeled amides *in vitro*, an approach that we refer to as azoline-mediated peptide backbone labeling (AMPL; Figure 1). The AMPL method has a broad substrate scope, including peptides lacking a N-terminal leader peptide, and can even be utilized to install backbone labels on large proteins with an appropriate substrate sequence. Furthermore, we demonstrate that this method is generalizable and can be carried out with divergent TOMM cyclodehydratases, facilitating the expansion of the methodology to diverse peptide scaffolds.

To explore the potential value of the AMPL method, we applied this labeling strategy to study substrate processing by TOMM cyclodehydratases. Previously we provided substantial, but indirect, support for a mechanism of cyclodehydration in which ATP is used to phosphorylate the carbonyl oxygen of the amide preceding the cyclized residue.<sup>23,24</sup> Through AMPL, we generated a cyclodehydratase substrate containing <sup>18</sup>O labels at these amides and used this substrate to provide direct evidence of a phosphorylated intermediate during TOMM cyclodehydrations. The AMPL method also proved generally useful for localizing azolines on cyclodehydratase-treated peptides. The lability of azoline heterocycles renders their detection by mass spectrometry challenging. While this can be overcome via

the addition of a dehydrogenase to convert the azoline heterocycles to stable azoles, TOMM clusters have been identified that lack a dehydrogenase,<sup>25</sup> preventing the universal application of this solution. Further, dehydrogenases have an inherent regio- and chemoselectivity, which can differ from the selectivity of the cyclodehydratase (see Figure S1).<sup>19,23</sup> The selective incorporation of <sup>18</sup>O labels into peptide backbones at the sites of azoline heterocycles using the AMPL method circumvents this pitfall. As a proof of principle, we utilized AMPL to localize azoline heterocycles on diverse *in vitro* cyclized substrates. More generally, we demonstrate that AMPL can be utilized for azoline heterocycle detection on natural products, which has the potential to assist in structure determination efforts.

## RESULTS AND DISCUSSION

### Oxygen isotope incorporation into peptide backbones through azoline hydrolysis

We reasoned that since azolines hydrolyze under even mildly acidic conditions to yield an amide bearing a solvent-derived oxygen,<sup>19</sup> performing the hydrolysis in [<sup>18</sup>O]-H<sub>2</sub>O would afford a peptide containing an <sup>18</sup>O-labeled carbonyl directly N-terminal to every hydrolyzed azoline heterocycle (Figure 1). During the initial characterization of the Balh cyclodehydratase (complex of BalhC and BalhD), it was discovered that cyclodehydration occurred unabated in the absence of the dehydrogenase.<sup>24</sup> We surmised that it would be possible to generate appropriately labeled substrates by first cyclizing the BalhA1 substrate and subsequently hydrolyzing the nascent rings in mildly acidic [<sup>18</sup>O]-H<sub>2</sub>O. To test this hypothesis, thioredoxin tagged-BalhA1 (Trx-BalhA1; Figure S2) was treated with BalhCD to afford the previously reported penta-azoline species (-90 Da; Figure 2a).<sup>24</sup> Following lyophilization to remove [<sup>16</sup>O]-H<sub>2</sub>O, the penta-azoline peptide was hydrolyzed in [<sup>18</sup>O]-H<sub>2</sub>O containing 0.5% (v/v) formic acid. As suspected, this treatment afforded a species with a mass 10 Da heavier than the starting material, suggesting that the substrate contained five <sup>18</sup>O-labels, [<sup>18</sup>O<sub>5</sub>]-BalhA1. Moreover, the mass increase was predicated on azoline formation, as both an unmodified peptide and a peptide containing oxidized azole heterocycles were inert under the hydrolysis conditions employed (Figure S3). This result was consistent with previous reports demonstrating that acid-catalyzed isotope exchange of carboxylic acids occurs slowly.<sup>26,27</sup> Following the removal of spent synthetase buffer, [<sup>18</sup>O<sub>5</sub>]-BalhA1 was subjected to a second treatment with BalhCD. As before, the peptide was modified to a penta-azoline state; however, ring formation was accompanied by a -100 Da mass shift, consistent with the loss of all five <sup>18</sup>O labels (Figure 2a). Fourier transform (FT) MS/MS was utilized to definitively localize the <sup>18</sup>O-labeled positions to the amides immediately N-terminal to the cyclized cysteines (Figure 2b).

### Thiolysis of oxazoline heterocycles allows for site-selective thioamide formation in peptide backbones

The conversion of amides into thioamides is commonly achieved through the use of thionation reagents (*e.g.* Lawesson's reagent).<sup>11,28</sup> Such treatments suffer from exceedingly poor site-selectivity and are not suitable for the modification of larger peptides.<sup>29,30</sup> An alternative strategy entails the thiolysis of an oxazoline heterocycle using H<sub>2</sub>S (*i.e.* sulfur nucleophile) for the site- and chemoselective formation of thioamides.<sup>31</sup> Based on this, we hypothesized that AMPL could be extended accordingly. For initial tests, we chose a simplified BalhA1 substrate derivative designed to form only a single oxazoline heterocycle, BalhA1<sub>NC</sub>-A40T (Figure S2). All other Cys/Ser and Thr residues in the core peptide of BalhA1 have been mutated to Ala and Val, respectively, and are thus non cyclizable (BalhA1<sub>NC</sub>). Following cyclodehydration by BalhCD, BalhA1<sub>NC</sub>-A40T was treated with potassium hydrosulfide (KHS; a solid, readily-handled alternative to H<sub>2</sub>S) and analyzed by mass spectrometry (Figure 3a). KHS treatment resulted in a 32 Da mass increase from the

cyclized peptide, consistent with oxazoline thiolysis. Importantly, no modification was seen if the oxazoline was not formed prior to KHS treatment (Figure S4). While these data indicated that thioamide formation had occurred, attempts to locate the modification site by LC-MS/MS failed due to incomplete fragmentation of the peptide (data not shown). To demonstrate selective thioamide incorporation, a minimal substrate, BalhX (Figure S2, *vide infra*), was subjected to thiolysis and subsequent LC-MS/MS analysis. As expected, the methyloxazoline on BalhX efficiently converted to a thioamide (Figure S5), and the modification could be definitively localized to the threonine heterocyclization site (Figure S6).

Previous reports on the relative reactivity of thiazolines and oxazolines towards nucleophiles demonstrated that the former is substantially less reactive.<sup>20-22</sup> To determine if this attenuated reactivity would preclude thiolysis of thiazoline heterocycles, an analogous study was carried out with BalhA1<sub>NC</sub>-A40C (Figure S2). The resultant spectra demonstrated that thioamide formation did not occur upon KHS treatment of the thiazoline heterocycle (Figure 3b). Attempts to promote thiolysis with higher concentrations of KHS, higher temperature, pH modulation, and longer reaction times all failed to generate the thioamide product (data not shown). Thus, under the conditions we employed, the AMPL-based thiolysis is remarkably chemoselective for (methyl)oxazoline heterocycles. As a further illustration of chemoselectivity, BalhA2 was converted to a tri-thiazoline, mono-oxazoline species by BalhCD and treated with KHS. As predicted, only a single thiolysis event was observed (Figure 3c). Previously, we have demonstrated that BcerB (dehydrogenase from a closely related TOMM cluster in *B. cereus*) was unable to oxidize oxazoline heterocycles.<sup>23</sup> As such, we predicted that treatment of BalhA2 with BcerB and BalhCD, coupled with subsequent thiolysis, would afford the tri-thiazole, mono-thioamide substrate. This was indeed the case, indicating that AMPL can be utilized for the synthesis of differentially functionalized peptides (Figure 3d).

### AMPL can be carried out on leader peptide-free substrates

An intriguing feature of ribosomally synthesized posttranslationally modified peptide (RiPP) natural product biosynthesis is the broad substrate tolerance of the modification enzymes.<sup>32-35</sup> While the basis of this promiscuity is under active investigation, it is well understood that the bipartite nature of the precursor peptides is a major contributor. RiPPs modification enzymes recognize substrates primarily through binding an N-terminal leader peptide. In contrast to the extensively modified C-terminal core region, the leader peptide does not undergo enzymatic processing.<sup>36</sup> Nonetheless, reports of leader peptide-independent RiPP processing enzymes have emerged.<sup>37</sup> For example, some lanthipeptide biosynthetic enzymes can process their substrates without the presence of the leader peptide, although the enzymatic activity is always higher when the leader peptide is supplied *in trans*.<sup>38-40</sup> Although a TOMM processing enzyme had not yet been reported to modify peptides without a leader peptide, we hypothesized that leader peptide-independent processing might be achievable with the substrate tolerant Balh synthetase.<sup>23</sup> To this end, a BalhA1 substrate derivative was generated lacking the leader peptide (BalhA1<sub>core</sub>; Figure S2) and modification by the Balh synthetase complex was assessed. Although modification by BalhCD alone generated the expected penta-azoline species, the addition of the dehydrogenase (BcerB) resulted in a complex mixture of oxidation products (Figure 4a). This was unexpected, as previous studies had demonstrated that cyclodehydration and oxidation were tightly coupled during BalhA1 processing,<sup>23,24</sup> and leader peptide binding was thought to be governed by the cyclodehydratase, not the dehydrogenase.<sup>16,41</sup> In an effort to promote more complete oxidation, the dehydrogenase concentration was doubled in a second reaction. The primary product, a tetra-azole, mono-azoline species (Figure S7), was subjected to MS/MS sequencing to localize the heterocycles. The fragmentation data

demonstrated that the cyclized positions were identical to the wild-type BalhA1 substrate and localized the single azoline to Cys20 (Cys45 in full-length BalhA1; Figure S2, S7). During BalhA1 processing, Cys45 is known to be the penultimate azole to be installed,<sup>23</sup> thus removing the leader peptide from the substrate appeared to disrupt both the order and efficiency of oxidation by the dehydrogenase.

While a decrease in oxidation rate suggested that substrate processing was dysregulated upon removal of the leader peptide, oxidation is not required for AMPL. To determine the effect of leader peptide removal on the rate of BalhA1<sub>core</sub> cyclodehydration, we carried out a purine nucleoside phosphorylase-coupled phosphate detection assay as previously described.<sup>23,24,42</sup> Attempts to determine the kinetic parameters for BalhA1<sub>core</sub> were unsuccessful, as it was not possible to saturate the enzyme with substrate. This result was in congruence with the well-established model of leader peptide-mediated substrate recognition.<sup>36</sup> As such, the initial velocity of BalhA1<sub>core</sub> processing at high substrate concentrations was compared to previously reported values for various substrate derivatives.<sup>23</sup> The data demonstrated that BalhA1<sub>core</sub> was modified at a slower rate than BalhA1 but at a rate comparable to the naturally occurring BalhA2 substrate (Figure 4b). The origin of the different processing rates for the naturally occurring BalhA1 and BalhA2 peptides derives from the presence of a Ser (Ser36), rather than the preferred Gly, immediately preceding the first cyclized residue (Cys37) in BalhA2.<sup>23</sup> As the  $K_M$  for BalhA1<sub>core</sub> was significantly larger than for BalhA2 (16  $\mu$ M), the similar processing reaction velocity between the two substrates requires that the intrinsically faster processing rate of BalhA1 ( $k_{obs} = 12.9 \text{ min}^{-1}$ ) be retained upon the leader peptide removal.<sup>23</sup>

To explore the generality of leader peptide-independent processing by the Balh synthetase, the modification of unnatural substrates was explored. Although not explicitly stated in the previous section, BalhX is a minimal substrate lacking a leader peptide (Figure S2). This 17-mer substrate contains a single heterocyclizable site that is cyclized by the Balh cyclodehydratase in route to thioamide formation (Figure S5). We observed that the modification efficiency of BalhX greatly improved upon the addition of leader peptide *in trans* (data not shown). This is reminiscent of studies with lanthipeptide modification machineries in which the leader peptide has been proposed to place the enzyme into an active conformation for substrate modification. In the case of the Balh cyclodehydratase, it remains unclear whether the addition of leader peptide *in trans* fulfills a similar role.

While modification of this simple 17-mer substrate demonstrated that leader peptide-independent processing was achievable on unnatural sequences, BalhX was still derived from the BalhA1 core peptide (see Figure S2). As such, the possibility remained that modification was due to inherent recognition of the core peptide by the Balh cyclodehydratase. Previous work demonstrated that the Balh synthetase can install azoles onto unnatural core peptides fused to the BalhA1 leader peptide.<sup>23</sup> One such chimeric substrate was the fusion of a truncated version of the McbA (microcin B17 precursor peptide) core peptide to the BalhA1 leader peptide (BalhA1-McbA). In order to test for leader peptide-independent conversion, wild-type McbA (Figure S2) was treated with BcerB and BalhCD. The resultant mass spectrum demonstrated that the Balh synthetase was able to modify the non-cognate McbA substrate (Figure S8), albeit with a decreased efficiency compared to reactions carried out with the chimeric BalhA1-McbA substrate.<sup>23</sup> In order to further assess the generality of the BalhCD leader peptide-independent activity, a similar reaction was carried out with a streptolysin S-like precursor peptide (SagX; Figure S2). As with the other substrates, treatment with the Balh synthetase resulted in modification of SagX (Figure S9). In the three aforementioned cases, the substrates contained heterocyclization sites that adhered to the previously reported Balh synthetase modification rules (Gly-Cys/Ser/Thr-Xaa, where Xaa = Pro).<sup>23</sup> To determine if these rules were retained

upon leader peptide removal, an additional three leader peptide-free substrates lacking Balh cyclodehydratase cyclization sites were reacted with BalhCD (Figure S10). In all cases, cyclodehydration was not observed indicating that the predictability of the Balh synthetase is retained upon leader peptide removal.

### Dehydrogenase-dependent synthetases can be engineered for compatibility with AMPL

In principle, AMPL could be carried out with any TOMM synthetase. However, of the six TOMM synthetases that have been reconstituted *in vitro*,<sup>14,15,23,43,44</sup> only the cyanobactin (PatD, patellamide; TruD, trunkamide) and Balh modification enzymes have been shown to function without the addition of the dehydrogenase.<sup>15,24</sup> The AMPL methodology is not inherently compatible with TOMM cyclodehydratases that function in a dehydrogenase-dependent fashion, as the azoline heterocycles synthesized by these synthetases are typically transformed to hydrolytically inert azoles. In the absence of a crystal structure of a TOMM synthetase, we posited that such dehydrogenase-dependent cyclodehydratases would likely require precise quaternary interactions in order to be competent catalysts; however, we reasoned that it would be quite unlikely that downstream azoline oxidation was required for efficient cyclodehydration. In order to co-opt a dehydrogenase-dependent cyclodehydratase for the production of only azoline heterocycles, we used bioinformatics to aid in the identification of conserved residues in TOMM dehydrogenases that were important for azoline oxidation. In an attempt to avoid mutations that may structurally destabilize the protein, positions predicted to be directly involved in FMN-binding were ruled out. By aligning divergent dehydrogenases, two highly conserved residues were identified that we hypothesized to be important for catalysis but not for FMN-binding (Figure S11). To test this hypothesis, we prepared two single-point mutants (K201A and Y202A) of the microcin B17 dehydrogenase (McbC), which has been long known to be required for cyclodehydration during microcin B17 processing.<sup>16</sup> Following purification, McbC-K201A and -Y202A were found to co-purify with FMN at levels similar to wild-type (Figure S12). As designed, the McbC-K201A and -Y202A permitted the production of azoline, but not azole, heterocycles when co-reacted with the Mcb cyclodehydratase (Figure 5). However, instead of converging to the known 9-azole form of McbA,<sup>45</sup> reactions carried out with the mutant dehydrogenases prematurely terminated after installing just two azolines. Due to the aforementioned lability of azolines, FT-MS/MS localization was not possible using standard methods (*vide infra*). Regardless, the use of this straightforward bioinformatics-guided strategy for conversion of dehydrogenase-dependent cyclodehydratases to azoline synthetases has the possibility to be a general strategy for synthetase repurposing.

### TOMM cyclodehydrations occur via an activated carbonyl intermediate

Recently, we utilized the Balh cyclodehydratase to provide evidence that ATP is utilized to directly phosphorylate the carbonyl oxygen involved in cyclization during azoline formation (Figure 6).<sup>24</sup> While this study demonstrated that ATP was hydrolyzed by a non-solvent, oxygen nucleophile, it did not directly confirm the proposed amide phosphorylation event. A more direct approach would be to perform cyclodehydration reactions with a substrate containing <sup>18</sup>O labels at every cyclized amide. In the event that direct activation was occurring, these <sup>18</sup>O labels would be found in the phosphate byproduct. However, due to the size of BalhA1 (57 residues; Figure S2), solid phase synthesis is impractical. While the generation of an appropriately labeled BalhA1 derivative could be achieved by native chemical ligation, this strategy would involve the synthesis and purification of two <sup>18</sup>O-labeled large peptide fragments (27 and 30 residues) and would be a tedious endeavor. Conversely, AMPL provides a convenient route to access labeled peptides such as [<sup>18</sup>O<sub>5</sub>]-BalhA1. Trx-tagged [<sup>18</sup>O<sub>5</sub>]-BalhA1, generated from azoline hydrolysis, was treated with BcerB/BalhCD and the isotopic constitution of the phosphate byproduct was analyzed by <sup>31</sup>P-NMR. A peak corresponding to [<sup>16</sup>O<sub>3</sub> <sup>18</sup>O]-phosphate (P<sub>i</sub>) was observed only in

reactions with [ $^{18}\text{O}_5$ ]-BalhA1 (Figure 6). Importantly, [ $^{16}\text{O}_3$   $^{18}\text{O}$ ]- $\text{P}_i$  was not detected in control reactions lacking enzyme or substrate.

While the detection of [ $^{16}\text{O}_3$   $^{18}\text{O}$ ]- $\text{P}_i$  provided strong support for the proposed phosphorylation mechanism, the detected amount of [ $^{16}\text{O}_4$ ]- $\text{P}_i$  was seemingly inconsistent with direct backbone activation being the sole mechanism of ATP utilization. We originally hypothesized that isotope scrambling with the ADP byproduct may be responsible for the [ $^{16}\text{O}_4$ ]- $\text{P}_i$  peak; however, a mass spectrum of ADP generated during the modification of [ $^{18}\text{O}_5$ ]-BalhA1 demonstrated that this was not the case (Figure S13). Although previous work demonstrated that the ATP/azole stoichiometry of the Balh cyclodehydratase is 1:1,<sup>24</sup> an alternative explanation was that ATP/azole stoichiometry was dysregulated for Trx-tagged [ $^{18}\text{O}_5$ ]-BalhA1 as a result of the requisite, extensive sample preparation. To test this, an identical reaction was carried out but the ATP/azole stoichiometry was measured rather than the  $\text{P}_i$  isotope distribution. Indeed, the stoichiometry assay showed that the previously reported 1:1 ratio of ATP/azole increased to 1.9:1 following the hydrolysis procedure. Taking into account the isotopic enrichment of [ $^{18}\text{O}_5$ ]-BalhA1 (Figure S14), the predicted [ $^{16}\text{O}_4$ ]- $\text{P}_i$ : [ $^{16}\text{O}_3$   $^{18}\text{O}$ ]- $\text{P}_i$  ratio is approximately 1.3:1. This result is in accord with the ratio observed by  $^{31}\text{P}$ -NMR. These data, obtained via reagents prepared by AMPL, provide strong evidence that cyclodehydration proceeds through a phosphorylated intermediate as previously proposed.<sup>24</sup>

### Azoline localization provides insights into TOMM cyclodehydratase substrate processing

The acid labile nature of azoline heterocycles has hindered their localization due to the acidic conditions often employed for efficient detection by mass spectrometry. As such, AMPL has the potential to aid in a variety of azoline biosynthetic studies by providing a rapid and robust method for azoline localization that takes advantage of acid lability, rather than suffering from it. To demonstrate the usefulness of such a strategy, we began by investigating azoline localization on BalhA2 (Figure S2). Upon BcerB/BalhCD treatment, BalhA2 was converted to a tri-azole, mono-azoline form (Figure 3d). While previous efforts localized the three azoles to the three N-terminal Cys residues, the azoline heterocycle could only be generally localized to a region of BalhA2 containing three heterocyclizable sites; Thr34, Thr35 and Ser36 (see Figure S2).<sup>23</sup> Through AMPL, we generated [ $^{18}\text{O}_4$ ]-BalhA2 and were able to definitively localize the fourth heterocycle to Thr34 using FT-MS/MS (Figure S15). This result is in accord with the known Balh cyclodehydratase selectivity rules (the residue N-terminal to Thr34 is Gly33).

Encouraged by the successful utilization of AMPL for identifying previously indeterminable sites of azoline formation, we returned our attention to the di-azoline McbA species generated from reactions containing McbBD and either McbC-K201A or -Y202A (Figure 4). Previous work on the order of ring formation in microcin B17 biogenesis demonstrated that the first two rings to be cyclized are Cys41 and Ser40, respectively.<sup>46</sup> With this in mind, we predicted that the two azolines installed on McbA in the mutant dehydrogenase assays would be located at the site of this bisheterocycle. However, a combination of iodoacetamide labeling (Figure S16) and the aforementioned  $^{18}\text{O}$ -labeling strategy coupled with FT-MS/MS, demonstrated that one of the cyclized residues was indeed Cys41, but that the other azoline was installed at either Cys48 or Cys51 (incomplete fragmentation between the two Cys precluded exact localization; Figure S17, S18). While it has been shown that both Cys48 and Cys51 can be installed on mutant substrates lacking the Ser of the first bisheterocycle site (Ser40A),<sup>47</sup> never before has a substrate with an intact, wild-type bisheterocycle site been observed to stop with only one of those heterocycles formed.<sup>46,48,49</sup> These results suggest that in microcin B17 biosynthesis, either the dehydrogenase controls the regioselectivity of the cyclodehydratase or that azoline oxidation is required for correct substrate processing. While our data cannot distinguish between these two possibilities, it

has been previously demonstrated that proper installation of the earlier rings is required for formation of the later rings, potentially through conformational control of the substrate.<sup>23,47</sup> As such, we favor a mechanism where azoline oxidation induces the requisite conformational restraints to facilitate modification of downstream residues. In this model, Cys41 would be heterocyclized first, but without oxidation, Ser40 is unable to be cyclized. This “roadblock” takes the cyclodehydratase off-pathway and results in the cyclization of a second Cys (either 48 or 51), at which point processing stalls. Although further study will be required to definitively determine the collaborating role that the dehydrogenase plays in cyclodehydration, these data provide yet another glimpse into the exquisite orchestration of substrate handling during TOMM biosynthesis and demonstrate the utility of the AMPL method.

As a final example of the usefulness of the AMPL method for azoline localization, we applied the method to a completely uncharacterized product. Previously, we demonstrated that BalhD is able to catalyze cyclodehydration in the absence of BalhC, albeit with a drastically reduced efficiency.<sup>24</sup> Although the role of BalhC was not explicitly interrogated, previous work on other TOMM synthetases has demonstrated that C proteins play an important role in substrate recognition.<sup>41</sup> If the C protein was required for proper substrate recognition, we hypothesized that the highly regulated order of azoline installation would be disrupted in reactions lacking BalhC. In order to test this hypothesis, BalhD-treated BalhA1 was subjected to the AMPL methodology to afford [<sup>18</sup>O<sub>2</sub>]-BalhA1, and the isotope labels were localized by FT-MS/MS. While one of the azolines was localized to Cys45, the second <sup>18</sup>O label was found at both Gly37 and Gly39, indicating that BalhD cyclized both Thr38 and Cys40 but not both simultaneously (Figure S19). In reactions containing BalhC, Cys40 is the first ring cyclized and Cys45 is the penultimate ring.<sup>23</sup> Moreover, the cyclization of Thr38 is unprecedented in reactions containing BalhC. Thus, these data suggest that BalhC is at least partially responsible for dictating the regio- and chemoselectivity of substrate processing by the Balh cyclodehydratase. Although additional roles for BalhC are possible,<sup>24</sup> the AMPL method provides a starting point for deconvoluting the roles of the individual proteins in the cyclodehydratase complex.

### Azoline stoichiometry of natural products through AMPL

The labeling of azoline heterocycles using selective hydrolysis is not restricted to *in vitro* reactions. In principle, the AMPL method for azoline labeling could be extended to determine the number and location of azoline rings on natural products. To demonstrate this, the azoline containing TOMMs plantazolicin, ulithiacyclamide, and lissocinamide 4 (Figure S1) were subjected to the AMPL method for <sup>18</sup>O-labeling. In all cases <sup>18</sup>O labeling was achieved (Figure S20-S22), demonstrating that AMPL can be utilized to derivatize both thiazolines and methyloxazolines on natural products. This suggests that the method could be generalized to provide the number and type (thiazoline vs. oxazoline) of azoline heterocycles in any natural product. Given that emerging natural products are most often available only in vanishingly small quantities, AMPL may prove valuable in assisting with the structural elucidation of these compounds.

## CONCLUSION

Prior to this work, the primary strategy for generating thioamides and oxygen isotope-labeled amides was SPPS. The method reported herein, which we refer to as azoline-mediated peptide backbone labeling (AMPL), provides the first chemoenzymatic strategy for accessing such derivatives. AMPL is compatible with both large and small peptides and peptide substrates fused to large proteins. Conveniently, labeling can be performed in the same pot as cyclodehydration, minimizing the amount of sample handling required during derivatization. In exploring the scope of AMPL, we have not only identified leader peptide-



independent processing by a TOMM cyclodehydratase, but also converted the naturally azole-producing Mcb synthetase into an azoline-only synthetase. Although our studies focused on the Balh and Mcb enzymes, AMPL can theoretically be applied to any TOMM synthetase, provided the enzymes can function independently of a dehydrogenase or the dehydrogenase can be inactivated without disrupting cyclodehydratase activity. The major limitation of the AMPL methodology is the inherent local sequence selectivity of the cyclodehydratase, which can be overcome by selecting the appropriate synthetase to modify a sequence of interest. As such, the *in vitro* reconstitution and characterization of additional TOMM cyclodehydratases will expand the sequence space accessible to the AMPL method.

In addition to providing a convenient strategy for generating polypeptides bearing unnatural amide derivatives, the utility of the AMPL method should also be of interest to enzymologists and natural products chemists, as we have used this labeling strategy to both investigate the mechanism of cyclodehydration and elucidate the localization of previously unresolvable heterocyclization sites. With respect to the former, our data have provided direct evidence that cyclodehydrations in RiPP natural products occur through the phosphorylation of the carbonyl oxygen immediately preceding the cyclized residue, which represents a novel use for ATP in biology. For the latter, we have focused our use of AMPL on identifying the location of enzymatically installed azoline heterocycles and through this simple labeling strategy have provided new insights into substrate processing by divergent TOMM cyclodehydratases. Furthermore, we demonstrate that the AMPL method can be extended to the modification of natural products, which opens up the possibility of using AMPL for both azoline-containing natural product discovery and structure elucidation.

## METHODS

### Protein overexpression and purification

Apart from the Trx-BalhA1 substrate used for the  $^{31}\text{P}$ -NMR study, all proteins were overexpressed as tobacco etch virus (TEV) protease- or thrombin-cleavable fusions to maltose-binding protein (MBP) and purified by amylose affinity chromatography as previously reported.<sup>24</sup> Unless otherwise stated, all reactions were carried out with tagged substrates and enzyme to avoid solubility issues.

### BalhA1 $^{18}\text{O}$ -labeling studies

Reactions containing 100  $\mu\text{M}$  MBP-BalhA1, 2  $\mu\text{M}$  MBP-BalhC/D and 0.2  $\mu\text{g/mL}$  TEV protease (to remove the MBP tags) were carried out in synthetase buffer [50  $\mu\text{M}$  Tris pH 7.5, 125 mM NaCl, 20 mM  $\text{MgCl}_2$ , 3 mM ATP, and 10 mM dithiothreitol (DTT)] at 25  $^\circ\text{C}$  for 18 h. Subsequently, the samples were frozen in liquid nitrogen, lyophilized to dryness to remove all [ $^{16}\text{O}$ ]- $\text{H}_2\text{O}$ , and the resultant solids were reconstituted to half of the initial volume with 97 atom % [ $^{18}\text{O}$ ]- $\text{H}_2\text{O}$ . To this solution, 10% formic acid in [ $^{16}\text{O}$ ]- $\text{H}_2\text{O}$  (v/v) was added to a final concentration of 0.5 % (v/v). This resulted in a final isotopic enrichment of ~92 atom %. Azoline hydrolysis was allowed to proceed for 18 h at 25  $^\circ\text{C}$ . The sample was then desalted via  $\text{C}_{18}$  ZipTip (Millipore) according to the manufacturer's instructions and  $^{18}\text{O}$  incorporation was analyzed on a Bruker Daltonics UltrafleXtreme MALDI-TOF spectrometer. Spectra were obtained in positive reflector mode using  $\alpha$ -cyano-hydroxycinnamic acid (CHCA) as the matrix. Control samples with either unmodified BalhA1 or fully oxidized BalhA1 (5 azoles instead of 5 azolines) were treated in an analogous fashion, except that MBP-BalhC/D were omitted or 2  $\mu\text{M}$  MBP-BcerB was added, respectively.

For the remodification of [ $^{18}\text{O}_5$ ]-BalhA1, the labeled substrate was  $\text{C}_{18}$  ZipTip desalted, to remove contaminating ADP and  $\text{P}_i$ , and subjected to a second treatment with fresh BalhC/D

under identical conditions to the initial reaction. Following an 18 h reaction at 25 °C, the sample was analyzed by MALDI-TOF MS as described above.

### FT-MS/MS localization of $^{18}\text{O}$ labels

Following azoline mediated  $^{18}\text{O}$  label incorporation, peptides were trypsin (sequencing grade, Promega) digested in 50 mM  $\text{NH}_4\text{HCO}_3$  (pH 8.0) for 30 min at 37 °C before quenching with formic acid at a final concentration of 10 % (v/v). Precipitate was removed via centrifugation at  $11,000 \times g$  and the samples were analyzed via reverse-phase, high-performance liquid chromatography-Fourier transform mass spectrometry (FT-MS). All FT-MS was carried out on an Agilent 1200 HPLC system with an autosampler connected directly to a Thermo Fisher Scientific LTQ-FT hybrid linear ion trap operating at 11 T. Separations were conducted using a  $1 \times 150$  mm Jupiter  $\text{C}_{18}$  column (300 Å, 5  $\mu\text{M}$ , Phenomenex) with 0.1 % formic acid (A) and acetonitrile containing 0.1 % formic acid (B) as the mobile phases. The LC gradient was held at 5 % B for 2 min before being increased to 50 % B over 43 min. All methods contained a full FT-MS scan followed by MS/MS of selected ions conducted in the FT. FT-MS scan parameters: minimal target signal counts: 5,000; resolution: 25,000;  $m/z$  range: variable. FT-MS/MS parameters: minimum target signal counts: 5,000; resolution: 25,000;  $m/z$  range: dependent on target  $m/z$ ; isolation width: 5  $m/z$ ; normalized collision energy: 35; activation q value: 0.25; activation time: 30 ms. Data analysis was conducted using the Qualbrowser application of Xcalibur v 2.2 (Thermo Fisher Scientific).

### $^{31}\text{P}$ -NMR analysis of phosphate isotope incorporation

$[\text{}^{18}\text{O}_5]$ -BalhA1 was generated in an identical strategy to the one described above except that 100  $\mu\text{M}$  Trx-BalhA1 was used instead of 100  $\mu\text{M}$  MBP-BalhA1 and the fusion tags were not removed. Following hydrolysis in  $[\text{}^{18}\text{O}]$ - $\text{H}_2\text{O}$ , all contaminating ADP and  $\text{P}_i$  was dialyzed from the sample by a 30,000-fold buffer exchange into storage buffer [50 mM Tris pH 7.5, 150 mM NaCl, 2.5 % glycerol (v/v)] using a 10 kDa Amicon Ultra centrifugal filtration unit (Millipore). Next, the phosphate concentration in the sample was measured by a malachite green phosphate detection assay (BioAssay Systems; supplemental methods) to ensure that the concentration of contaminating  $\text{P}_i$  was below 4  $\mu\text{M}$ . The concentration of Trx- $[\text{}^{18}\text{O}_5]$ -BalhA1 was determined both by the 280 nm absorbance and the Bradford colorimetric assay (Thermo Scientific). Reactions for  $^{31}\text{P}$ -NMR were carried out with 50  $\mu\text{M}$  Trx- $[\text{}^{18}\text{O}_5]$ -BalhA1 and 2  $\mu\text{M}$  MBP-tagged BCD in low-salt synthetase buffer (50 mM Tris pH 8.5, 25 mM NaCl, 5 mM  $\text{MgCl}_2$ , 10 mM DTT, and 2 mM ATP) for 3 h at 25 °C. Subsequently, the sample was quenched by the addition of 500 mM ethylenediaminetetraacetic acid (EDTA; pH 8.5) to a final concentration of 5 mM.  $\text{D}_2\text{O}$  was added to a final concentration of 10 % and the sample was transferred to a  $\text{D}_2\text{O}$ -matched Shigemi NMR tube. The  $^{31}\text{P}$ -NMR spectrum was obtained on a 600 MHz Varian Unity Inova NMR with a 5 mm Varian AutoTuneX probe, 1000 transients, 32768 points, and a spectral window of -15 to 5 ppm.

The identity of the  $[\text{}^{16}\text{O}_4]$ - $\text{P}_i$  peak was verified by spiking the reaction with  $\text{K}_2\text{PO}_4$  (pH 8.5) at a final concentration of 200  $\mu\text{M}$  and collecting a  $^{31}\text{P}$ -NMR spectrum under identical conditions. A control reaction with unlabeled Trx-BalhA1 was carried out in an identical manner, except that the initial azoline hydrolysis event was carried out in  $[\text{}^{16}\text{O}]$ - $\text{H}_2\text{O}$ .

### Processing of leader peptide-free substrates

100  $\mu\text{M}$  MBP-BalhA1<sub>core</sub> was reacted with 10  $\mu\text{M}$  MBP-tagged BalhC/D, either with or without 10  $\mu\text{M}$  MBP-BcerB, and 0.2  $\mu\text{g}/\text{mL}$  TEV protease in synthetase buffer for 18 h at 25 °C. Samples were then desalted and analyzed by MALDI-MS as above. Processing of the unnatural substrates, MBP-SagX, MBP-McbA, and BalhX, were carried out in an analogous

fashion with the following minor variations: all substrate concentrations were reduced to 50  $\mu\text{M}$ , proteolytic cleavage in the MBP-McbA sample was carried out using 0.02  $\mu\text{g/mL}$  thrombin (from bovine plasma), and MBP-tagged BalhA1 leader peptide was added to the BalhX sample at a final concentration of 50  $\mu\text{M}$ .

### Rate of BalhA1<sub>core</sub> processing

The rate of MBP-BalhA1<sub>core</sub> processing was determined using slight modifications to a previously described method.<sup>24</sup> Briefly, MBP-BalhC and MBP-BalhD were added to a cuvette for a final concentration of 1  $\mu\text{M}$  each. Reactions were initiated via the addition of a mixture of 100  $\mu\text{M}$  MBP-BalhA1<sub>core</sub>, 200  $\mu\text{M}$  2-amino-6-mercapto-7-methylpurine riboside (Berry and Associates), and 0.2 units of purine nucleotide phosphorylase in synthetase buffer at 25 °C. Reaction progress was monitored by the change in absorbance at 360 nm on a Cary 4000 UV-vis spectrophotometer (Agilent). Initial rates of phosphate production were calculated based on the linear absorbance change during the first 3 min of the reaction and the extinction coefficient of the resulting guanine analog (11,000  $\text{M}^{-1}\text{cm}^{-1}$ ). Error is reported as the standard deviation of the mean ( $n = 3$ ).

### Mcb synthetase reactions

20  $\mu\text{M}$  MBP-McbA was reacted with 1  $\mu\text{M}$  MBP-tagged McbB/D and either WT, K201A or Y202A McbC in synthetase buffer for 18 h at 25 °C. Reactions were initiated by the removal of MBP with the addition of 0.02  $\mu\text{g/mL}$  thrombin. As above, heterocycle formation was monitored after desalting by MALDI-MS. A control sample lacking McbC was treated in an identical fashion.

### Thiolysis of azoline heterocycles

Heterocyclization reactions of MBP-BalhA1<sub>NC</sub>-A40T and -A40C were carried out with 50  $\mu\text{M}$  substrate and 1  $\mu\text{M}$  MBP-BalhC/D in synthetase buffer for 18 h at 25 °C. For BalhX modification, the enzyme concentration was increased to 10  $\mu\text{M}$  and MBP-tagged BalhA1 leader peptide was added *in trans* to a final concentration of 50  $\mu\text{M}$ . In the A40T and A40C samples, MBP was proteolytically removed by the addition of 2  $\mu\text{g/mL}$  TEV protease. To each of samples, the proper volume of a fresh 1 M solution of potassium hydrosulfide (KHS; Strem Chemicals) was added to achieve a final concentration of 100 mM KHS, and thiolysis was allowed to proceed for an additional 18 h at 25 °C. The samples were then desalted and analyzed by MALDI-MS as above. For each substrate, a control reaction lacking MBP-BalhC/D was also subjected to thiolysis.

For reactions with BalhA2, 50  $\mu\text{M}$  MBP-tagged substrate was incubated with 1  $\mu\text{M}$  MBP-BalhC/D with and without 1  $\mu\text{M}$  MBP-BcerB. MBP was removed via the addition of 2  $\mu\text{g/mL}$  TEV protease. Following an 18 h reaction at 25 °C, the samples were treated with KHS and analyzed by MALDI-TOF MS as above.

## Supplementary Material

Refer to Web version on PubMed Central for supplementary material.

## Acknowledgments

We are grateful to Joel Melby for assistance with collecting MS/MS data, Eric Schmidt (University of Utah) for the generous gift of ulithiacyclamide and lissoclinamide 4, and members of the Mitchell lab for the critical review of this manuscript. This work was supported by the US National Institutes of Health (NIH) (1R01 GM097142 to D.A.M.). K.L.D. was supported by the University of Illinois Department of Chemistry Harold R. Snyder Fellowship. The Bruker UltrafleXtreme MALDI TOF/TOF mass spectrometer was purchased in part with a grant from the National Center for Research Resources, National Institutes of Health (S10 RR027109 A).

## REFERENCES

- (1). Wong A, Beevers AJ, Kukol A, Dupree R, Smith ME. *Solid State Nucl. Magn. Reson.* 2008; 33:72. [PubMed: 18502619]
- (2). Torres J, Briggs JA, Arkin IT. *J. Mol. Biol.* 2002; 316:365. [PubMed: 11851344]
- (3). Mukherjee P, Kass I, Arkin IT, Zanni MT. *Proc. Natl. Acad. Sci. U.S.A.* 2006; 103:3528. [PubMed: 16505377]
- (4). Ihalainen JA, Paoli B, Muff S, Backus EH, Bredenbeck J, Woolley GA, Cafilisch A, Hamm P. *Proc. Natl. Acad. Sci. U.S.A.* 2008; 105:9588. [PubMed: 18621686]
- (5). Shim SH, Gupta R, Ling YL, Strasfeld DB, Raleigh DP, Zanni MT. *Proc. Natl. Acad. Sci. U.S.A.* 2009; 106:6614. [PubMed: 19346479]
- (6). Lemaitre V, de Planque MR, Howes AP, Smith ME, Dupree R, Watts A. *J. Am. Chem. Soc.* 2004; 126:15320. [PubMed: 15563125]
- (7). Hu J, Chekmenev EY, Gan Z, Gor'kov PL, Saha S, Brey WW, Cross TA. *J. Am. Chem. Soc.* 2005; 127:11922. [PubMed: 16117514]
- (8). Bartlett PA, Spear KL, Jacobsen NE. *Biochemistry.* 1982; 21:1608. [PubMed: 7082637]
- (9). Choudhary A, Raines RT. *Chembiochem.* 2011; 12:1801. [PubMed: 21751326]
- (10). Batjargal S, Wang YJ, Goldberg JM, Wissner RF, Petersson EJ. *J. Am. Chem. Soc.* 2012; 134:9172. [PubMed: 22468862]
- (11). Goldberg JM, Batjargal S, Petersson EJ. *J. Am. Chem. Soc.* 2010; 132:14718. [PubMed: 20886849]
- (12). Goldberg JM, Speight LC, Fegley MW, Petersson EJ. *J. Am. Chem. Soc.* 2012; 134:6088. [PubMed: 22471784]
- (13). Seyfried MS, Lauber BS, Luedtke NW. *Org. Lett.* 2010; 12:104. [PubMed: 20035564]
- (14). Li YM, Milne JC, Madison LL, Kolter R, Walsh CT. *Science.* 1996; 274:1188. [PubMed: 8895467]
- (15). McIntosh JA, Donia MS, Schmidt EW. *J. Am. Chem. Soc.* 2010; 132:4089. [PubMed: 20210311]
- (16). Milne JC, Roy RS, Eliot AC, Kelleher NL, Wokhlu A, Nickels B, Walsh CT. *Biochemistry.* 1999; 38:4768. [PubMed: 10200165]
- (17). Sivonen K, Leikoski N, Fewer DP, Jokela J. *Appl Microbiol Biotechnol.* 2010; 86:1213. [PubMed: 20195859]
- (18). Duan L, Wang S, Liao R, Liu W. *Chem. Biol.* 2012; 19:443. [PubMed: 22520750]
- (19). Molohon KJ, Melby JO, Lee J, Evans BS, Dunbar KL, Bumpus SB, Kelleher NL, Mitchell DA. *ACS Chem. Biol.* 2011; 6:1307. [PubMed: 21950656]
- (20). Martin RB, Parcell A. *J. Am. Chem. Soc.* 1961; 83:4835.
- (21). Martin RB, Parcell A. *J. Am. Chem. Soc.* 1961; 83:4830.
- (22). Martin RB, Hedrick RI, Parcell A. *J. Org. Chem.* 1964; 29:3197.
- (23). Melby JO, Dunbar KL, Trinh NQ, Mitchell DA. *J. Am. Chem. Soc.* 2012; 134:5309. [PubMed: 22401305]
- (24). Dunbar KL, Melby JO, Mitchell DA. *Nat. Chem. Biol.* 2012; 8:569. [PubMed: 22522320]
- (25). Donia MS, Ravel J, Schmidt EW. *Nat. Chem. Biol.* 2008; 4:341. [PubMed: 18425112]
- (26). Niles R, Witkowska HE, Allen S, Hall SC, Fisher SJ, Hardt M. *Anal. Chem.* 2009; 81:2804. [PubMed: 19243188]
- (27). Stewart II, Thomson T, Figeys D. *Rapid Commun. Mass Spectrom.* 2001; 15:2456. [PubMed: 11746917]
- (28). Pedersen U, Thorsen M, Elkhisy EEAM, Clausen K, Lawesson SO. *Tetrahedron.* 1982; 38:3267.
- (29). Brown DW, Campbell MM, Walker CV. *Tetrahedron.* 1983; 39:1075.
- (30). Lajoie G, Lepine F, Maziak L, Belleau B. *Tetrahedron Lett.* 1983; 24:3815.
- (31). Wipf P, Miller CP, Venkatraman S, Fritch PC. *Tetrahedron Lett.* 1995; 36:6395.
- (32). Donia MS, Hathaway BJ, Sudek S, Haygood MG, Rosovitz MJ, Ravel J, Schmidt EW. *Nat. Chem. Biol.* 2006; 2:729. [PubMed: 17086177]

- (33). Tianero MD, Donia MS, Young TS, Schultz PG, Schmidt EW. *J. Am. Chem. Soc.* 2012; 134:418. [PubMed: 22107593]
- (34). Li B, Sher D, Kelly L, Shi Y, Huang K, Knerr PJ, Joewono I, Rusch D, Chisholm SW, van der Donk WA. *Proc. Natl. Acad. Sci. U.S.A.* 2010; 107:10430. [PubMed: 20479271]
- (35). Haft DH, Basu MK, Mitchell DA. *BMC Biol.* 2010; 8:70. [PubMed: 20500830]
- (36). Oman TJ, van der Donk WA. *Nat. Chem. Biol.* 2010; 6:9. [PubMed: 20016494]
- (37). Dunbar KL, Mitchell DA. *ACS Chem. Biol.* 2013; 8:473. [PubMed: 23286465]
- (38). Levengood MR, Patton GC, van der Donk WA. *J. Am. Chem. Soc.* 2007; 129:10314. [PubMed: 17676843]
- (39). Oman TJ, Knerr PJ, Bindman NA, Velasquez JE, van der Donk WA. *J. Am. Chem. Soc.* 2012; 134:6952. [PubMed: 22480178]
- (40). Wang H, van der Donk WA. *ACS Chem. Biol.* 2012; 7:1529. [PubMed: 22725258]
- (41). Mitchell DA, Lee SW, Pence MA, Markley AL, Limm JD, Nizet V, Dixon JE. *J. Biol. Chem.* 2009; 284:13004. [PubMed: 19286651]
- (42). Webb MR. *Proc. Natl. Acad. Sci. U.S.A.* 1992; 89:4884. [PubMed: 1534409]
- (43). Lee SW, Mitchell DA, Markley AL, Hensler ME, Gonzalez D, Wohlrab A, Dorrestein PC, Nizet V, Dixon JE. *Proc. Natl. Acad. Sci. U.S.A.* 2008; 105:5879. [PubMed: 18375757]
- (44). Gonzalez DJ, Lee SW, Hensler ME, Markley AL, Dahesh S, Mitchell DA, Bandeira N, Nizet V, Dixon JE, Dorrestein PC. *J. Biol. Chem.* 2010; 285:28220. [PubMed: 20581111]
- (45). Sinha Roy R, Kelleher NL, Milne JC, Walsh CT. *Chem. Biol.* 1999; 6:305. [PubMed: 10322125]
- (46). Kelleher NL, Hendrickson CL, Walsh CT. *Biochemistry.* 1999; 38:15623. [PubMed: 10569947]
- (47). Roy RS, Allen O, Walsh CT. *Chem. Biol.* 1999; 6:789. [PubMed: 10574779]
- (48). Kelleher NL, Belshaw PJ, Walsh CT. *J. Am. Chem. Soc.* 1998; 120:9716.
- (49). Belshaw PJ, Roy RS, Kelleher NL, Walsh CT. *Chemistry & Biology.* 1998; 5:373. [PubMed: 9662507]

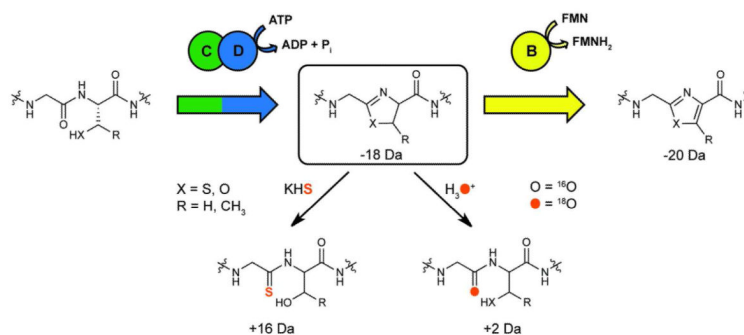


**Figure 1.**

Azoline heterocycles are versatile intermediates for selective peptide labeling. A general scheme for TOMM heterocycle biogenesis is displayed. Select Cys, Ser, and Thr residues are cyclized by the ATP-dependent cyclodehydratase (complex of C and D proteins). Azoline heterocycles can then be oxidized by a flavin-dependent dehydrogenase to afford the aromatic azole. Alternatively, the electrophilic azoline heterocycle can be exploited for the installation of oxygen isotopes and thioamides using [ $^{18}O$ ]-H<sub>2</sub>O and potassium hydrosulfide (KHS) as nucleophilic ring-opening agents, respectively. The mass shift relative to unmodified peptide is displayed underneath each product.

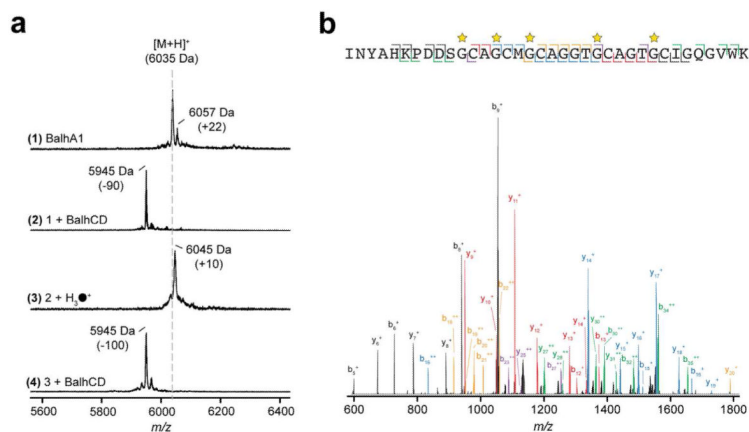


**Figure 2.**

Site-specific incorporation of <sup>18</sup>O labels into BalhA1. **(a)** An overlay of MALDI-TOF MS spectra displaying the <sup>18</sup>O exchange process. Mass labels correspond to the 1+ charge state and all mass shifts are reported relative to the pertinent non-cyclized species (spectra 1 and 3). The loss of the <sup>18</sup>O labels in [<sup>18</sup>O<sub>5</sub>]-BalhA1 upon retreatment with BalhCD is evidenced by the loss of 100 Da (compared to -90 Da for BalhA1). <sup>18</sup>O labels are represented by filled circles. **(b)** The FT-MS/MS spectrum of trypsin digested [<sup>18</sup>O<sub>5</sub>]-BalhA1. The b and y ions are colored based on the number of <sup>18</sup>O labels present in the fragment (green, 5; purple, 4; orange, 3; blue, 2; red, 1; black, 0). Stars represent the location of the <sup>18</sup>O labels.

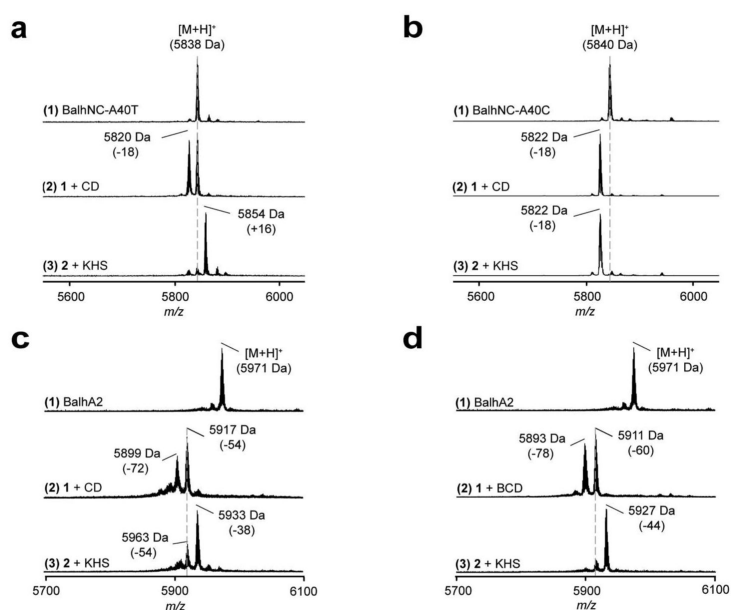


**Figure 3.** Thiolysis is specific for oxazoline heterocycles. MALDI-TOF MS overlays showing the thiolysis of (a) BalhA1-NC-A40T, (b) BalhA1-NC-A40C, (c) BalhA2 treated with the cyclodehydratase (CD), and (d) BalhA2 treated with both the cyclodehydratase and the dehydrogenase (BCD) are displayed. Mass labels correspond to the 1+ charge state and all mass shifts are reported relative to the pertinent unmodified species (spectrum 1).



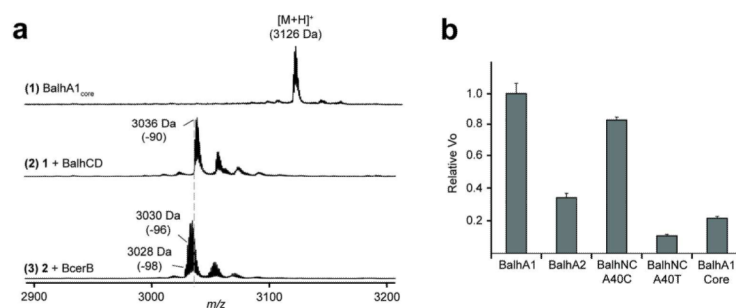


**Figure 4.** BalhA1<sub>core</sub> processing. **(a)** An overlay of MALDI-TOF MS spectra displaying BalhCD- and BcerB/BalhCD-treated BalhA1<sub>core</sub>. Mass labels correspond to the 1+ charge state and all mass shifts are reported relative to the unmodified species (spectrum 1). **(b)** Relative processing rates for previously reported leader peptide-containing substrates of BalhCD are displayed alongside the processing rate for BalhA1<sub>core</sub>. Error bars represent standard deviation from the mean (n = 3).

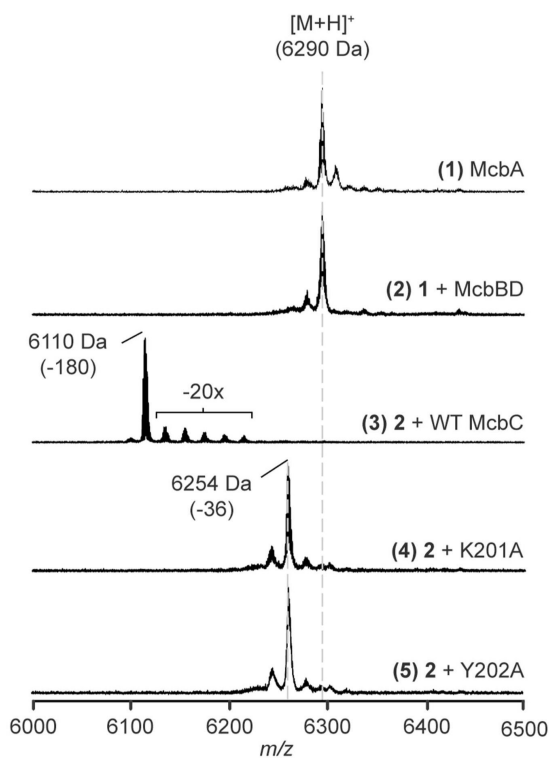


**Figure 5.**

Azoline formation by the microcin B17 synthetase. An overlay of MALDI-TOF spectra displaying McbA processing by the Mcb cyclodehydratase (McbBD) with either wild-type (WT) or the mutant (K201A, Y202A) Mcb dehydrogenases (McbC) is shown. Mass labels correspond to the 1+ charge state and all mass shifts are reported relative to the unmodified species (spectrum 1). In the WT McbC reaction (spectrum 3), partially processed intermediates with 5-8 azoles (labeled -20x) are seen in addition to the fully modified, 9-azole substrate.

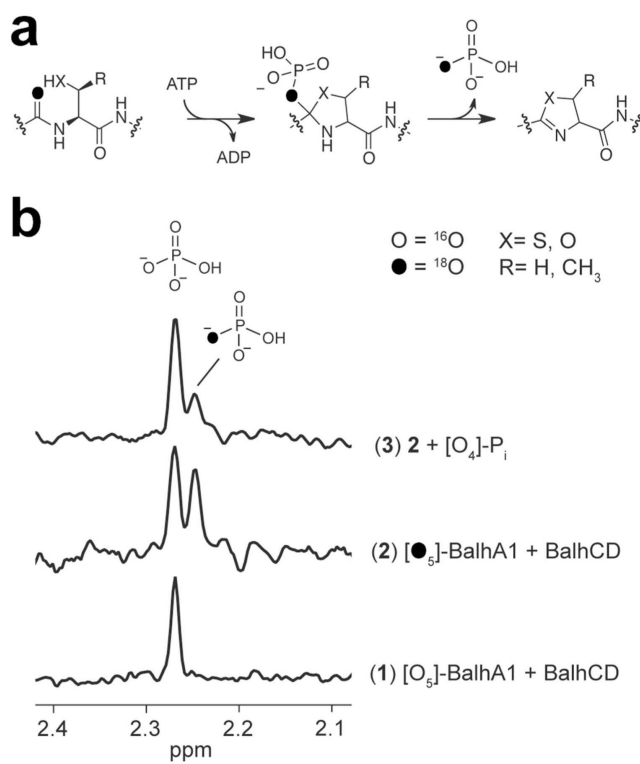


**Figure 6.** <sup>31</sup>P-NMR of <sup>18</sup>O<sub>5</sub>-BalhA1 reactions. (a) The putative carbonyl oxygen phosphorylation mechanism for ATP utilization is displayed along with <sup>31</sup>P-NMR spectra from both [<sup>18</sup>O<sub>5</sub>]-BalhA1 and [<sup>16</sup>O<sub>5</sub>]-BalhA1 reactions (b). The identity of the [<sup>16</sup>O<sub>4</sub>]-P<sub>i</sub> peak was verified by spiking the sample with a P<sub>i</sub> standard (spectrum 3).